Report JET1 November 2021 The Group of Plasma Theory

VI.3. Identification of the control parameters of the impurity pinch and of the main scaling laws of the transport coefficients using the DNS and the DTM codes

1. Introduction

One of the problem of present-day tokamak devices such as JET [1] or AUG [2] is that of heavy impurity accumulation at the center of the plasma. The phenomenon is especially relevant for tungsten (W) impurities resulting from the erosion of plasma facing components. A peculiar transport mechanism comes in play and drives W ions from the SOL region towards the core of the tokamak where they become an intense channel of energy-loss via photon emission. When the relative concentration of tungsten at the center of the plasma reaches $\sim 10^{-4} - 10^{-3}$ the fusion process can be even stopped. This scenario will remain relevant for the ITER project [3] in which tungsten will still be used for the coating of plasma facing components.

In previous stages of this project (the main Reports of 2017 and 2018) we have identified and described a novel mechanism, hidden drifts [4], of inward radial transport relevant for W ions. The hidden drifts are quasi-coherent elements of motion in the stochastic dynamics of ions in turbulent plasmas which, in special conditions, can lead to an effective velocity identified as radial pinch. The conditions required for this phenomenon to happen are: the existence an effective poloidal velocity field and a symmetry breaking mechanism represented by compressible effects. In a plasma, the effective poloidal velocity field can be identified as the result of diamagnetic drifts or plasma rotation. The compressible effects that were taken into account were the polarization drift [5] and the parallel acceleration [6]. Numerical simulations of both cases confirmed the existence of the radial pinch within simple transport models (reports of 2018 and 2020).

In the present stage of the project we intend to offer a quantitative description of these intimate mechanisms of radial pinch. This will be achieved using a more refined transport model that includes collisions, neoclassical drift and both polarization and parallel acceleration. The model is tackled from a statistical perspective using test particles while the turbulence is represented within the direct numerical simulation method as an ensemble of stochastic fields with known Eulerian statistics. With this numerical tool at hand, extensive simulations will be carried out to investigate the dependency of the radial pinch on the parameters of the model. In this way the control parameters will be identified.

2. The transport model

We consider a simple, axisymmetric, model of the magnetic field which in simple toroidal coordinates (r, θ, ζ) reads:

$$\boldsymbol{B} = \frac{B_0 R_0}{R}\left(\hat{\boldsymbol{e}}_\zeta + b_\theta(r)\hat{\boldsymbol{e}}_\theta\right)$$

With R_0 the major radius of the tokamak and $R = R_0 + r\cos\theta$. Starting from this structure one can define a set of field-aligned coordinates described by the versors:

$$\hat{\boldsymbol{e}}_\parallel = \frac{\hat{\boldsymbol{e}}_\zeta + b_\theta(r)\hat{\boldsymbol{e}}_\theta}{\sqrt{1+b_\theta^2}}, \qquad \hat{\boldsymbol{e}}_\perp = \frac{\hat{\boldsymbol{e}}_\theta - b_\theta(r)\hat{\boldsymbol{e}}_\zeta}{\sqrt{1+b_\theta^2}}, \quad \hat{\boldsymbol{e}}_r$$

The trajectory of the guiding-center of an impurity ion is described by the phase-space: $(\boldsymbol{x}, v_\perp, v_\parallel)$. The equations of motion describe the associated dynamics are standard drift velocities, in agreement with gyro-kinetic theories [ ]:

$$\begin{cases} \dfrac{d\boldsymbol{x}}{dt} = \boldsymbol{V}_\phi + \boldsymbol{V}_D + \boldsymbol{\eta} + V_p\hat{\boldsymbol{e}}_\theta + \dfrac{v_\parallel \boldsymbol{B}}{B} \\ \dfrac{v_\perp dv_\perp}{dt} = \dfrac{v_\perp^2}{2}\left(v_\parallel \dfrac{\nabla B\cdot\boldsymbol{B}}{B^2} + \dfrac{\nabla\phi\cdot(\nabla B\times\boldsymbol{B})}{B^3}\right) \\ \dfrac{\mathrm{v}_\parallel dv_\parallel}{dt} = -\dfrac{v_\perp dv_\perp}{dt} - \nabla\phi\cdot\dfrac{d\boldsymbol{x}}{dt} \end{cases}$$

The terms in the first equation can be identified as $\boldsymbol{V}_\phi$ the ExB and polarization drift, $\boldsymbol{V}_D$ the magnetic and curvature drift, $\boldsymbol{V}_p$ the poloidal velocity and $\boldsymbol{\eta}$ the collisional velocity:

$$\begin{cases} \boldsymbol{V}_\phi = -\nabla\phi\times\dfrac{\boldsymbol{B}}{B^2} + \boldsymbol{u}_p \\ \boldsymbol{u}_p = -\dfrac{\partial_t\nabla\phi}{\Omega\,\mathrm{B}} \\ \boldsymbol{V}_D = -\dfrac{Am}{Ze}\left(\dfrac{v_\perp^2}{2} + v_\parallel^2\right)\dfrac{\nabla\mathrm{B}\times\boldsymbol{B}}{B^3} \end{cases}$$

Dimensionless quantities specific to the turbulent transport are used. The units are: the Larmor radius of the protons $\rho_i = \frac{v_{th}}{\Omega_i}$ (for the radial and perpendicular displacements, for the correlation lengths $\lambda_r, \lambda_\perp$ for $\frac{1}{k_0}$ and for the corresponding wave numbers), the small radius of the plasma a (for the parallel distances and for the correlation length $\lambda_\parallel$), $\tau_0 = \frac{a}{v_{th}}$ (for time and for τ_c), A_ϕ (for the potential ϕ), $V_\star = \frac{\rho_i v_{th}}{a}$ (for the radial and perpendicular velocities and V_p), $D_0 = \frac{\rho_i^2}{\tau_0}$ (for the perpendicular diffusion) and $v_{thW} = v_{th}\sqrt{A}$ where $v_{th} = \frac{T_i}{m_p}$ is the thermal velocity of protons with temperature T_i and mass m_p, and $\Omega_i = \frac{eB}{m_p}$ is the cyclotron frequency of the protons. The equations of motion written in scaled field-aligned coordinates $x = \boldsymbol{x}\hat{e}_r - r_0, y = r\boldsymbol{x}\hat{e}_\theta, z = R\boldsymbol{x}\hat{e}_\zeta$ read:

$$\frac{dx}{dt} = \frac{K_\star\left(-\partial_y\phi + C_A\partial_{tx}\phi\right)(R_0^2 - r^2)}{(R_0 - r\cos\chi)(R_0 + r_0)} - P_m\left(\frac{v_\perp^2}{2} + v_\parallel^2\right)\frac{(\sin\chi)}{\left(1 - \frac{r}{R_0}cos\,\chi\right)\sqrt{1 + b_\theta^2(r)}} + P_c\eta_r(t)$$

$$\frac{dy}{dt}=\frac{K_\star\left(+\partial_x\phi+C_A\partial_{ty}\phi\right)(R_0^2-r^2)}{(R_0-r\cos\chi)(R_0+r_0)}$$
$$-P_m\left(\frac{v_\perp^2}{2}+v_\parallel^2\right)\left(\frac{\cos\chi}{\left(1-\frac{r}{R_0}cos\,\chi\right)\sqrt{1+b_\theta^2(r)}}-\frac{2r}{1-r^2}-\frac{R_0b_\theta b_\theta'}{1+b_\theta^2(r)}\right)+P_c\eta_y(t)$$
$$+\frac{V_p}{\sqrt{1+b_\theta^2(r)}}$$

$$\frac{v_\perp dv_\perp}{dt}=\frac{v_\perp^2}{2}\frac{\rho_i}{R_0}\left[-\left(\frac{\cos\chi}{\left(1-\frac{r}{R_0}cos\,\chi\right)\sqrt{1+b_\theta^2(r)}}-\frac{2r}{1-r^2}-\frac{R_0b_\theta b_\theta'}{1+b_\theta^2(r)}\right)\frac{dx}{dt}+\frac{sin\chi}{1-r\,cos\chi}\frac{dy}{dt}\right]$$

$$\frac{v_\parallel dv_\parallel}{dt}=-\frac{v_\perp dv_\perp}{dt}-Z\Phi\left(\frac{\partial\phi}{\partial x}\frac{dx}{dt}+\frac{\partial\phi}{\partial y}\frac{dy}{dt}+\frac{\partial\phi}{\partial t}\right)-P_{acc}\frac{\partial\phi}{\partial z}v_\parallel$$

The parameters of the model are captured in the non-dimensional constants:

$$K_\star=\frac{\Phi a}{\rho_i},\ \Phi=\frac{eA_\phi}{T_i},\ C_A=\frac{A}{Z}\frac{\rho_i}{a},\quad P_{acc}=\frac{\Phi Z}{\sqrt{A}},\quad P_m=\frac{1}{Z}\frac{a}{R_0}.$$

3. The direct numerical simulation method

The plasma turbulence is represented within our model by the electrostatic field ϕ which is considered to be a stochastic random field with known Eulerian corelation $E(\boldsymbol{x},t)=\langle\phi(\boldsymbol{x},t)\phi(0,0)\rangle$. The same is true for the collisional velocities which are stochastic by nature and can be described by the correlation function $C_r(t)=\langle\eta_r(t)\eta_r(0)\rangle$. The statistical approach to the problem of transport is the following: a statistical ensemble of random fields $\{\phi,\eta_r,\eta_\perp\}$ are considered to drive an associated ensemble of trajectories $(\boldsymbol{x}=(x,y,z),v_\perp,v_\parallel)$ accordingly with the transport model described in the previous section. With these trajectories, transport coefficients can be computed as Lagrangian averages: $D_r(t)=\langle x(t)v_x(0)\rangle, V_r(t)=\langle v_x(t)\rangle$. Further details on the statistical approach can be found in a previous work [7].

Furthermore, within the direct numerical simulation method [7], we choose specific representations of the random fields in terms of random waves:

$$\phi(x,y,z,t)=c\sum_i^{N_c}\sin\left(k_x^ix+k_y^iy+k_z^iz-\omega^it+\alpha^i\right)$$

$$\eta_r(t) = c\sum_i^{N_c} sin(\omega_c^i t + \alpha_r^i)$$

$$\eta_\perp(t) = c\sum_i^{N_c} sin(\omega_c^i t + \alpha_\perp^i)$$

where the four-vectors $k_i, \omega_i = (k_x^i, k_y^i, k_z^i, \omega^i)$ are randomly distributed, with the PDF $S(k,\omega)$. The same is true for the frequencies ω_c^i which are randomly distributed with the PDF $S_c(\omega_c)$. The phases $\alpha_i, \alpha_\perp^i, \alpha_r^i \in (0,2\pi]$ are uniformly generated and c is a mere normalization constant $c = 2/N_c$. Using the central limit theorem it can be shown that the fields become Gaussian in the limit $N_c \to \infty$. We consider here drift type turbulence, which has a specific spectrum S(k, ω) that can be modeled in accordance with the experimental measurements and numerical calculations [5,6]:

$$S(k,\omega) = S_x(k_x)S_y(k_y)S_z(k_z)S_\omega(\omega)$$

$$S_x(k_x) = \frac{\lambda_x}{\sqrt{2\pi}} e^{-\frac{k_x^2\lambda_x^2}{2}}, \quad S_z(k_z) = \frac{\lambda_z}{\sqrt{2\pi}} e^{-\frac{k_z^2\lambda_z^2}{2}}$$

$$S_y(k_y) = \frac{\lambda_x k_y}{2k_0\sqrt{2\pi}}\left(e^{-\frac{(k_y-k_0)^2\lambda_y^2}{2}} - e^{-\frac{(k_y+k_0)^2\lambda_y^2}{2}}\right)$$

$$S_\omega(\omega) = \frac{\tau_c}{2\pi}\left(\frac{1}{1+\tau_c^2(\omega+\omega_0)^2} + \frac{1}{1+\tau_c^2(\omega-\omega_0)^2}\right)$$

Which corresponds to the correlation function:

$$E(x,y,z,t) = A_\phi^2 \frac{\partial}{\partial y}\left(e^{-\frac{x^2}{2\lambda_x^2}-\frac{y^2}{2\lambda_y^2}-\frac{z^2}{2\lambda_z^2}} \frac{\sin(k_0 y)}{k_0} e^{-\frac{t}{\tau_c}} cos(\omega_0 t)\right)$$

Similarly for the collisional velocities:

$$S_c(\omega_c) = \frac{1}{\pi\, \nu}\left(\frac{1}{1+\nu^2\omega_c^2}\right)$$

$$C(t) = e^{-t\nu}$$

We note that the method is exact in principle its only limitation being numerical by nature: N_c the number of partial waves used in the expansion of the fields and N_p the number of elemenets in the statistical ensemble should be infinite. In turn we use finite values $N_c \sim 10^3$ and $N_p \sim 10^5$ since it was found that such values provide enough statistical convergence both at Eulerian and Lagrangian levels. From a numerical perspective we solve the eqns. Of the model using a 4-th order Runge-Kutta method with a constant time step $\Delta t = 0.1\min(\lambda_\perp/K_\star, \nu^{-1}, \tau_c)$ for a time interval $t_{max} = 5\max(\tau_c, 1/\nu)$ yielding a number of timesteps N_t.

4. Results and control parameters

In the framework of the transport model described in section 1.2 and within the statistical representation provided by the direct numerical simulation model (section 1.3) we performed extensive numerical simulations. These simulations were done considering a basic configuration of the tokamak and of the turbulence. Around this configuration, several physical parameters were varied.

We consider the case of a tokamak device has a major radius $R/\rho_i = 1500$ and the minor radius $a/\rho_i = 300$. The turbulence amplitude $A_\phi/T_i = 0.03$, the correlation lengths $\lambda_x = 5, \lambda_y = 2, \lambda_z = 1, k_0 = 1$. The correlation times $\tau_c = 10, \nu^{-1} = 5$ and the drift frequency $\omega_0 = 1$. The poloidal velocity expresset in terms of diamagnetic $V_\star$ is taken $V_p = 1$. Considering a W ion with $A = 184$, an average ionization rate $Z = 40$ and an ion thermal energy $E = T_i$ which translates in the following values of the scaled parameters:

$$K_\star = 15,\ \Phi = 0.03,\ C_A = 0.09,\quad P_{acc} = 0.09,\quad P_m = 0.0083.$$

In order to get a more sensible understanding of how different components of motion affect the transport, we separate the problem in two limits: AP ($C_A = 0$) and PDP ($P_{acc} = 0$).

One of the important parameters of the model which distinguishes between various heavy ions is the charge ionization Z. In this respect we choose to study the two limits described above and simulate the transport model for different values of $Z \in (10,70)$. The resulting values of the inward pinch are presented in Fig. 1. One can observe two dependencies: the AP pinch increases monotonically, almost linearly with Z while the PDP decreases monotonically, almost parabolically with Z. This can be easily understood looking at the parameters P_{acc} and C_A which control the magnitude of the parallel acceleration and polarization drift. While $P_{acc} \propto Z$, the second parameter $C_A \propto 1/Z$ thus, the radial pinch is roughly proportional with these parameters. In the limit of large ionization states the polarization drift has almost no effect on the radial pinch while the converse is true for the parallel acceleration. From the intersection of the curves we conclude that an intermediate value of ionization is best suited for the minimization of the inward transport.

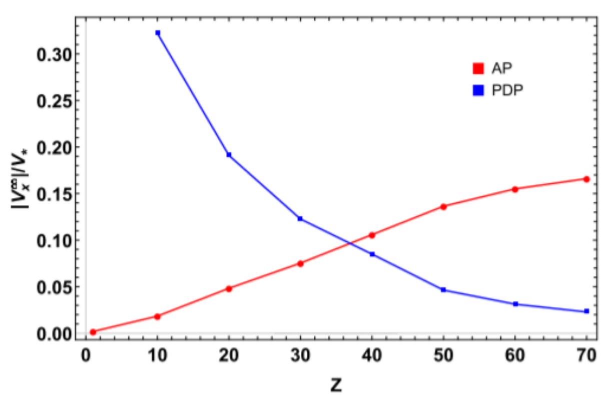

Fig. 1: . The asymptotic velocities $|V_x^\infty|$ as functions of Z for the PDP (blue) and for the AP (red) for $\Phi = 0.03$ and $V_p = 1$.

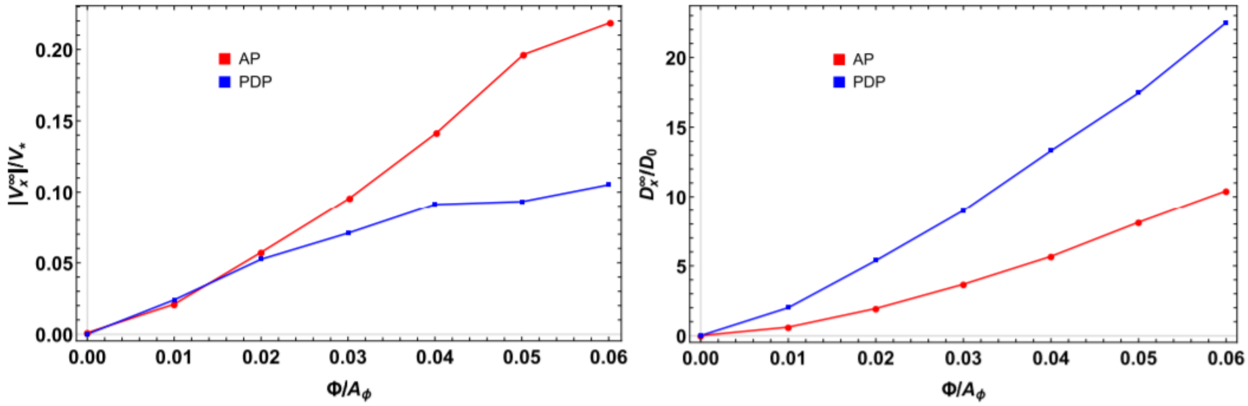

Fig.2: The dependence on the amplitude Φ of asymptotic velocities $|V_x^\infty|$ (left panel) and of the diffusion coefficient D_x^∞ for the PDP (blue) and for the AP (red). $Z = 40 \; and \; V_p = 1$.

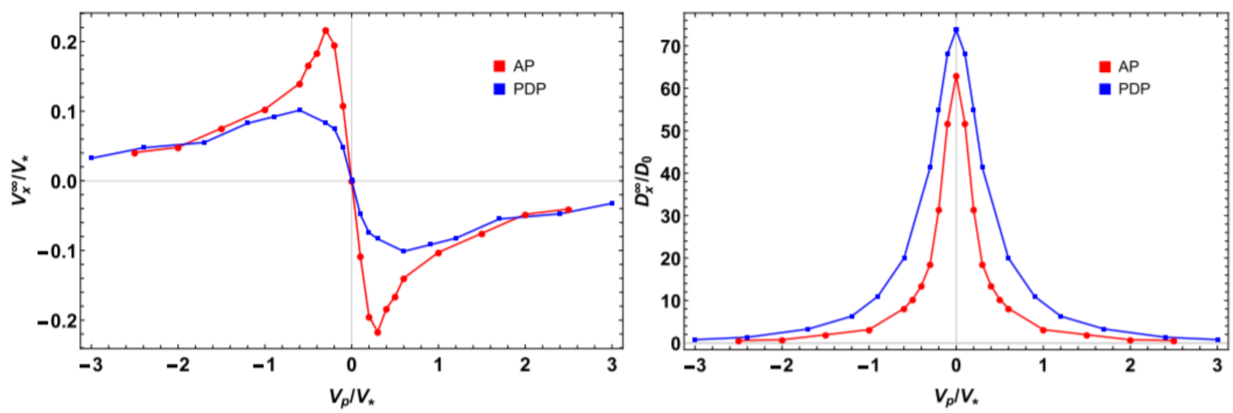

Fig. 3: The dependence on the poloidal velocity V_p of asymptotic velocities V_x^∞ (left panel) and of the diffusion coefficient D_x^∞ for the PDP (blue) and for the AP (red). $\Phi = 0.03, and \; Z = 40$.

We take a step further and investigate the effects of turbulence amplitude on both the radial inward pinch and the radial diffusion. The results are presented in Fig. 2 for both limiting case. As expected, the turbulence amplitude has an almost linear increasing effect on theV_x^∞. The diffusion for the other hand exhibits a peculiar superdiffusive behaviour since D_x^∞ grows faster than linear. Obviously, turbulence is an efficient mechanism of control, mitigating diffusion resulting in a decrease in radial transport.

We gather our results in the following estimations of the main dependences of the radial transport coefficients on the control parameters:

$$\begin{cases} |V_x^\infty| \sim \frac{1}{Z}, PDP \\ |V_x^\infty| \sim Z, AD \end{cases}, \qquad \begin{cases} |V_x^\infty| \sim \frac{V_p}{a+V_p^2}, PDP + AD \\ |D_x^\infty| \sim \frac{1}{1+V_p^2}, \;\; PDP + \; AD \end{cases}, \qquad \begin{cases} |V_x^\infty| \sim \Phi, PDP + AD \\ |D_x^\infty| \sim \Phi^{1.2}, \;\; PDP + \; AD \end{cases}$$

Conclusion

We have used a complex transport model for the description of impurity dynamics in tokamak turbulent plasmas. The model includes **ExB**, polarization, magnetic and diamagnetic drifts, collisions, parallel acceleration and neoclassical effects. The transport coefficients are extracted from the statistical approach of test particles moving accordingly with the transport model in an ensemble of stochastic random fields. The latter are modelled in the framework of direct numerical simulation method. Two relevant transport coefficients are computed: the radial diffusion and the radial velocity pinch. Extensive simulations are performed for a variety of parameters of the model and the main control parameters are identified. These are the poloidal velocity, turbulence amplitude and impurity effective charge. Specific scaling laws were determined and analytically approximated.

References

[1] Neu, V. Bobkov, R. Dux, A. Kallenbach, T. P¨utterich, H. Greuner, O. Gruber, A. Herrmann, C. Hopf, K. Krieger et al., J. Nucl. Mater. 363–365, 52 (2007).

[2] Valisa M. et al (JET-EFDA Contributors) 2011 Nucl. Fusion 51, 033002

[3] https://www.iter.org/

[4] M. Vlad, F. Spineanu, 2018 EPL 124 60002

[5] M. Vlad, F. Spineanu, Physics of Plasmas 25, 092304 (2018)

[6] M. Vlad, D. I. Palade, F. Spineanu, *Plasma Phys. Control. Fusion* **63** 035007 (2021)

[7] D.I.Palade, M.Vlad, Statistics and Computing volume 31, Article number: 60 (2021)

[8] Vlad M., Spineanu F., Phys. Plasmas 22, 112305 (2015).

[9] Vlad M., Spineanu F., Nuclear Fusion 56, 092003 (2016).

[10] Philipps V. 2011 Tungsten as material for plasma-facing components in fusion devices J. Nucl. Mater. 415 S2R

VI.4 Neoclassical effects on the turbulent advection of heavy impurities in the presence of alpha particles

1. Introduction

During H mode there is neoclassical and turbulent inward flow of heavy (high- Z) impurities. The NBI-sustained part of the current density is modified by the change in local Z_{eff} (via stronger electron friction) and can even reverse direction relative to NBI. On the other hand the bootstrap current due to alpha particles from DT reactions is unidirectional and also affected by the presence of heavy impurities. These two contributions can change the profile of the current density $j(r)$ in the central region of plasma. When there is accumulation of high- Z impurities the profile of $j(r)$ can become similar to the one of the reversed shear (RS or Enhanced RS) regimes. The current density has a radial interval of increase, a hump and then a decay toward the edge . This is equivalent to formation on a finite radial interval of a cuasi-flat profile for the safety factor $q(r)$ before it rises again toward the edge. Two effects are connected with this very low magnetic shear $\widehat{s} = r(dq/dr)/q \ll 1$: (1) the drift waves are linearly more stable since the radiative condition (Pearlstein Berk 1969) toward the ion turning points actually assumed a linear in r magnetic shear around the resonance surface; (2) elements of plasma driven by the radial convection across this radial interval will preserve the vorticity (for relatively uniform particle density) because of the generalized Ertel's theorem. Further another global invariance, of the kinetic helicity, will generate a compensating vorticity layer of opposite sign. This is favorable to the formation of an Internal Transport Barrier.

The sequence of connections mentioned above generates a state similar with the "reversed shear" with however a possible important role of the accumulation of heavy impurities. Therefore it is transient to the extent to which the radiation will limit the H mode.

The objective is the formulation of a consistent physical picture of these processes and the estimation of the effect of high-Z impurities and of the alpha's bootstrap on the velocity shear and implicitly on the Internal Transport Barrier formation.

2. The NBI current drive and the influence of the impurities

The electric current determined by the NBI is due to the momentum transfer to the background particles, ions and electrons. If the transfer of momentum from the fast NBI ions to the background particles would lead to an equal flow of ions and electrons then it would be no new electric current. Actually both background ions and background electrons that have received momentum in the direction of injection undergo collisional friction with other plasma particles and this is different for the two species. Electrons collide with background ions and with impurity ions (in particular high- Z) and lose the momentum obtained from the fast NBI ions at a rate that is different of the loss (friction) rate of the ions. In addition the trapped electrons have an effect on the flow of electrons. Then the flow (current) of electrons in the direction of injection is different of that of ions. For counter injection the total NBI current contribution can be negative. It is said that the current driven by the NBI is reversed.

The current is

$$j = |e| n_b v_b - j^{elec}$$

For $j^{elec} = -\int d^3 v [e] v f_e^{(1)}$ and $f_e = F_{Me} + f_e^{(1)}$. Equation for the collisional effects on the electrons $(b \equiv \text{beam})$ is Fokker Planck with only neoclassical drift [1], [2]

$$v_{\parallel} \frac{B_\theta}{B_T} \frac{\partial f_e^{(1)}}{r \partial \theta} - \frac{m_e}{e} v_{\parallel} \frac{\partial}{r \partial \theta} \left(\frac{v_{\parallel}}{B} \right) \frac{\partial}{\partial r} F_{Me} = C[\text{beam} \rightarrow e, i]$$

The collision term (RHS) has the following content. $C_{eb}[F_{Me}, f_b]$ represents collisions with the NBI ions, which imprints a motion in the direction of beam; $C_{ei}[f_e', F_{Mi}]$ represents collisions with the thermal ions, a friction force; collisions with the electrons $C_{ee}\left[f_e^{(1)}, F_{Me}\right] + C_{ee}\left[F_{Me}, f_e^{(1)}\right]$, which have both effects: transfer momentum from the energized electrons to the background electrons, which is a friction, and also induce supplementary flow.

Solving for the distribution function for the electrons $f_e^{(1)}$, allows to calculate the current of electrons

$$j_e = -e \int d^3 v \; v_{\parallel} \; f_e^{(1)}.$$

The momentum that is obtained by the background ions is the momentum lost by the beam (b) ions

$$m_i n_i u_i + m_b n_b u_b = 0.$$

The current carried by the ions is

$$j_i = eZ_b\ n_b u_b - eZ_i\ n_i u_i = eZ_b n_b u_b \left(1 - \frac{m_b Z_i}{m_i Z_b}\right).$$

Now, for the current carried by the electrons, one has to solve the kinetic equation. To calculate $C_{e,b}$ one must replace the hot distribution function $f_{b,0}$ in the Rosenbluth potentials. Using $h = 1 + \varepsilon \cos\theta$ and $\varepsilon = r/R$, $\eta = \sqrt{1 - \frac{v_\perp^2}{v^2}(h-\varepsilon)}$ it is introduced the usual separation of variables, with $w \equiv \frac{v^2}{2}$, and for $\eta \sim 1$

$$f_{b,0} = \sum_{n=0}^{\infty} a_n(w)\ P_n(\eta).$$

The solutions for the kinetic equations for beam ions and for the electrons have been obtained an a series of papers by Cordey, Start, Houghton, Jones [1 – 3]. The total current can be expressed as [3]

$$j = e\ n_b\ u_b Z_b \\ \times \left\{1 - \frac{Z_b}{Z_i} + 1.46\sqrt{\varepsilon}\left(\frac{Z_b}{Z_i} - \frac{Z_i}{Z_b}\frac{m_b}{m_i}\right)\ A(Z_i)\right\},$$

where A is an expression derived from the collisional operator, which has the magnitude of the order 1 (between 1 and 1.6).

The net current is in the opposite direction relative to the beam for $Z_b = 1$ and $v_b^* = v_b/v_e \sim 1.3$.

We learn from this analytical calculation that the contribution from the NBI to the total current density can be opposite (reversed current) when there are high- Z impurities.

3. The bootstrap current of the α particles

In the spirit of the present idea, the NBI current, strongly influenced by the high- Z impurities and the bootstrap current of the α particles combine to produce a particular modulation of the current density profile. This can lead to the creation of the conditions that there is a region with approximately quasi-flat profile of the safety factor $q(r)$, similar to the Reversed Shear (RS) regime. We need to calculate the contribution of the bootstrap from the α 's.

The current is derived on the basis of the force balance (averaged over magnetic surface) which involves the gradient of the pressure (anisotropic: parallel and perpendicular) and friction. All species: α 's, background ions, electrons and impurities interact by collisions. The Fokker Planck equation describes the transfer of momentum and energy from α 's to electrons and ions [4]

The equation for the α function $f_\alpha^{(0)} + \overline{f}_\alpha$ is

$$v_\parallel \nabla_\parallel \left(\overline{f}_\alpha + I\frac{v_\parallel}{\Omega_\alpha}\frac{\partial}{\partial\psi} f_\alpha^{(0)} - v_\parallel V_{\parallel i}^* \frac{\partial}{\partial w} f_\alpha^{(0)}\right) + \frac{Z_\alpha e}{m_\alpha} v_\parallel E_\parallel^* \frac{\partial}{\partial w} f_\alpha^{(0)} \\ = \frac{1}{\tau_s}\left[\frac{1}{2} v_b^3 \frac{\partial}{\partial v} \cdot U \cdot \frac{\partial}{\partial v}\overline{f}_\alpha + \frac{\partial}{\partial v}\cdot\left(1 + \frac{v_c^3}{v^3}\right) v \overline{f}_\alpha\right] (\mathrm{coll}) \\ + \frac{S}{4\pi v^2}\delta(v - v_0)\ \ (\mathrm{source})$$

where $U = (v^2 I - vv)/v^3$. Separating the neoclassical drift part and the the velocity shift part, one defines $\overline{f}_\alpha = f_{\alpha 1} + P$, the distribution function for the alpha particles is, to first order of neoclassical theory

$$f_{\alpha 1} = -\frac{I v_\parallel}{\Omega_\alpha}\frac{\partial}{\partial \psi} f_{\alpha 0} + v_\parallel V_{\parallel i}^{*}\frac{\partial}{\partial w} f_{\alpha 0} + P(\lambda, w, \psi)$$

The first term $\frac{I v_\parallel}{\Omega_\alpha}\frac{\partial}{\partial \psi} f_{\alpha 0} \approx \rho_\theta |\nabla f_{\alpha 0}|$ is the usual neoclassical correction due to particle drift. The second comes from the part in the Maxwell exponential $-\frac{(v_\parallel - V_i^*)^2}{2T/m} \sim -\frac{2 v_\parallel V_i^*}{2T/m} \sim \frac{v_\parallel V_i^*}{w}$. The last term P contains neoclassical and collisional effects and if finite for circulating and zero for trapped. The source is $f_\alpha^{(0)}(\psi, v) = \frac{S}{4\pi(v^2 + v_c^3)} \tau_s H(v_0 - v)$ where H is the Heaviside function, v_0 is the inital velocity of a α particle, v_c is the critical velocity separating the regimes of energy transfer (drag) dominated by electrons and respectively ions, v_b represents the pitch angle scattering of α 's by the background ions. The part P of the distribution function is expressed as a sum over the "forces" and "fluxes" and the separation of variables w and λ in velocity space is used to exploit the eigenfunctions of the collision operator

$$P(\lambda, w, \psi) = \sum_{j=1,2,3}\left(\sum_{n=1}^{\infty} \Lambda_n(\lambda, \psi) V_{nj}(w, \psi)\right) A_j(w, \psi)$$

The function $P(\lambda, w, \psi)$ is the distribution function that is zero in the trapped region. Its expression contains the "forces" A_j i.e. the gradients of the equilibrium distribution in real space and in velocity space; and the conjugated "fluxes" V_{nj} that can be found by solution of the Fokker Planck equation similar to the NBI case. Also, $\Lambda_n(\lambda, w)$ are the eigenfunctions of the pitch angle scattering operator. The notations $w \equiv \frac{v^2}{2}$, $\lambda \equiv \frac{v_\perp^2}{v^2} h$, $h \equiv \frac{B_0}{B} = 1 + \frac{r}{R}\cos\theta$, $I \equiv B \cdot R^2 \nabla\phi \simeq R B_T$. Definition of the ion parallel flow

$$V_{\parallel i}^{*} = -\frac{I}{n_i m_i \Omega_i}\frac{\partial}{\partial \psi} p_i + K_i B$$

where the first term is the usual diamagnetic velocity and K_i is from the poloidal velocity $K_i \equiv V_i \cdot \frac{\nabla\theta}{B \cdot \nabla\theta}$

The driving forces for $P(\lambda, w, \psi)$ are $A_{1,2,3}$ given in terms of gradients in real and velocity space of $f_{\alpha 0}$ The electric acceleration on the interval between two collisions (τ_s) is $\sim \tau_s |e| E_\parallel v_\parallel \frac{1}{T_e} f_{e0} F_{ei}^{Spitzer}$, where $\frac{1}{T_e} f_{e0} F_{ei}^{Spitzer} \rightarrow \frac{\partial}{\partial \varepsilon} f$. The Spitzer problem is included by $E_\parallel^* = E_\parallel - \frac{Z_\alpha}{n_i |e|} F_{\parallel ei}$.

The conjugated fluxes $V_{n1,2,3}$ are determined using the same analytic calculations as for the NBI fast ions. Using A_j and V_{nj} one calculates the distribution function $f_{\alpha 1}$ and then the current. This contains the series which is P and now this can be made explicit. The electron-ion collisions still have to be calculated with the collision operator that includes the effect of impurities $\nu_{ei} = \nu_{ei}^{(0)}\left(1 + \frac{n_\alpha Z_\alpha^2}{n_e Z_{eff}}\right)$. From this, the parallel relative velocity between electron and ions becomes (with the usual B modulation and averaged on surface)

$$\langle V_{ie\parallel} B\rangle = \left\langle V_{ie\parallel}^{(0)} B\right\rangle \left[1 + O\left(\frac{n_\alpha Z_a^2}{n_e Z_{eff}}\right)\right] - \left(1 - F_\mu^i\right)\frac{n_\alpha Z_a^2}{n_e Z_{eff}} \langle V_{\alpha i\parallel} B\rangle$$

where $F^{e,i,\alpha} \equiv$ effective fraction of trapped electrons, respectively of ions and of α 's. They are determined in terms of ν_{ei} , ν_{ee} and the α collisions. The bootstrap current induced by alphas is [4], [5]

$$\frac{\langle J_{bs}^{\alpha}\ B\rangle}{B_0} = \left(1 - \frac{Z_\alpha}{Z_{eff}}\left(1 - F_\mu^e\right)\right) F_\mu^\alpha \left(-\frac{I}{B_0}\frac{\partial}{\partial\psi} p_\alpha\right)$$

This formula exhibits the influence of the high- Z impurities on the α 's bootstrap.

5. Plasma rotation and Internal Transport Barrier

We return to our physical picture where the accumulation of high- Z impurities plays a role in the formation of the ITB in reversed shear configurations.

The combination between the current generated by the NBI and the bootstrap current density sustained by alpha particle leads to a particular radial profile for the current density. When the heavy impurities are accumulated in the central area the two contributions, each with particular dependence on the Z_{eff} can produce a modification of the current profile that is favorable for confinement.

The profile of the current density shows a flat central region, a hump for greater r and then the usual radial decay toward the edge value. The safety profile is reversed i.e. decays from the center and has a radial interval where it is almost flat, before rising again toward the edge value. A flat $q(r)$ means that the drift waves have smaller rate of excitation. However the radial flow of heat is very large and is both conductive and convective, since it is sustained by NBI and alpha heating. The convective aspect is a possible reference to the Rayleigh Benard (RB) random "plume" convective events, which are considered the source of the "wind" and has previously been examined as a possible explanation for the L to H transition. In the present case this would correspond to the Internal Transport Barrier. The thermal convection events, analogous to the "plumes" in RB induce poloidal rotation (the "wind") which means vorticity oriented mainly along the toroidal direction, $\boldsymbol{\omega} = \omega \widehat{\mathbf{e}}_\phi$, with $\omega = \nabla \times v$ and $\mathbf{v} = v_\theta \widehat{\mathbf{e}}_\theta$, ω is dominated by the poloidal velocity shear $\partial v_\theta / \partial r$.

We remind that the vorticity, the poloidal magnetic field (i.e. the safety factor) and the particle density are involved in the Lagrangian invariance [6] expressed by the generalized Ertel's theorem $\frac{d}{dt}\left(\frac{\omega + \alpha B + \Omega_{ci}}{n}\right) = 0$.

The cuasi-flat profile (for a finite radial interval) of $q(r)$ has the consequence that the convective elements of plasma will preserve their vorticity, i.e. to a cuasi-flat profile of $q(r)$ corresponds a cuasi-flat profile of ω . Then the invariance of the kinetic helicity

$$K = \int d^2 r\ \boldsymbol{\omega} \cdot \boldsymbol{v} = \quad \mathrm{const}$$

requires a compensating opposite vorticity contribution, in the form of a layer of poloidal sheared rotation, which will act as an Internal Transport Barrier. The physical process that effectively makes possible this compensation (and conservation of K) is the Hinton's thermal instability, explained below.

Note. We also note that, from

$$\frac{-|\omega|}{\Omega_{ci}} + \frac{\varepsilon^2}{2q^2} \sim \mathrm{const} \times n$$

[6] it results that, when $|\omega|$ is larger on a zone which is off-axis, then q must have a minimum in that region, in order the two terms (of opposite sign) to compensate their change and the sum to remain approximately constant. This is compatible with the reversed- q profile, i.e. with what we claim can result from the high- Z impurity accumualtion.

The strong thermal component of the plasma balance in the region where $q(r)$ is almost flat suggests the "thermal bifurcation" model of Hinton [7]. This model is purely neoclassical and is based on the equilibrium poloidal velocity sustained by the gradient of the temperature

$$u_\theta = -\frac{1}{eB}\mu_i \frac{\partial T_i}{\partial r}$$

(here $\mu_i = 0.7$ for Pfirsch Schluter and changes sign for lower collisionality). The coefficient is a function of ion collisionality. The variation of the temperature is reflected in the variation of this coefficient and these are the premises for an instability. The sequence is actually a favorable evolution of this instability.

Initially there is a poloidal rotation of the plasma, with a velocity that is proportional with the gradient of the temperature. Large flux of heat (both conduction and convection, from NBI and alphas) have three effects (1) increase the gradient of the temperature; correspondingly, the poloidal velocity is higher; (2) modify the physical coefficient that connects the gradient of temperature to the poloidal velocity, because the ion collisionality decreases; since there is spatial variation of the temperature, the poloidal velocity becomes strongly sheared; and (3) since the temperature is high, the parallel viscosity (the mechanism for magnetic pumping damping of poloidal rotation) is weak and is subject to the nonlinear decrease according to the theory of Shaing and Crume.

The result is a transport barrier and the gradient of the temperature continue to increase, with the three consequences listed above.

6. Relation with experiment

The RS and ERS are known to be favorable confinement regimes. It is also known that the Internal Transport Barrier is formed at the rational surface corresponding to the minimum of $q(r)$. The model that we have developed here is intended to reveal the role of the accumulation of the high- Z impurities in the reversed $q(r)$ profile.

Quantitatively the alpha's bootstrap can be around 10% of the boostrap current from the background ions. It can be reduced by the presence of impurities by a percent of approx. 20% when $Z_{eff} \sim 2.5$.

Assuming that the density is almost uniform in the center, in that region an approximation is

$$|\omega| q^2 \approx \text{const} \times r^2$$

Then if the vorticity is higher off-axis, the factor q must be reduced, which is compatible with our reversed q profile induced by high- Z impurities.

Taking $\Omega_{ci} \sim 10^8\ (s^{-1})$, $\varepsilon^2 \sim 0.1$ we have from $\frac{|\omega|}{\Omega_{ci}} \sim \frac{\varepsilon^2}{2q^2}$ the estimation $|\omega| \sim \frac{10^7}{2q^2}$. If the velocity varies with an amount of $\delta v \sim 10^5\ (m/s)$ on a distance of $1\ (cm)$ then $\omega \sim 10^7\ (s^{-1})$ and the orders of magnitude are reasonable $q \sim 1$. These data are compatible with the experimental observation of the ITB revealed as a layer of poloidal rotation of C^{IV} in DIII-D [8].

References

[1] D.F.H. Start, J.G. Cordey, Phys. Fluids 23 (1980) 1477

[2] D.F.H. Start, J.G. Cordey, E.M. Jones, Plasma Physics 22 (1980) 303

[3] J.G. Cordey, E.M. Jones, D.F.H. Start, A.R. Curtis, I.P. Jones, Nuclear Fusion 19 (1979) 249

[4] C. T. Hsu, K. C. Shaing, R. P. Gormley, and D. J. Sigmar, Phys. Fluids B4 (1992) 4023.

[5] C. T. Hsu, P. J. Catto, and D. J. Sigmar, Phys. Fluids B2 (1990) 280.

[6] F. Spineanu and M. Vlad, Nucl. Fusion 56 (2016) 092005.

[7] F.L. Hinton, Phys. Fluids B 3, (1991) 696.

[8] M.E. Austin et al., Phys. Plasmas 13, (2006) 082502.

Acknowledgement

This work has been carried out within the framework of the EUROfusion Consortium and has been received funding from the European Union’s Horizon 2020 research innovation programme under grant agreement number 633053 and also from the Romanian National Education Minister under contract 2/23.02.2016. The reviews and opinion expressed herein do not necessarily reflect those of the European Commission.

Papers

[1] M. Vlad, D.I. Palade, F. Spineanu, Effects of the parallel acceleration on heavy impurity transport in turbulent tokamak plasmas, *Plasma Phys. Control. Fusion 63, 035007 (2021)*

[2] D. I. Palade, Turbulent transport of fast ions in tokamak plasmas in the presence of resonant magnetic perturbations, *Physics of Plasmas 28, 022508 (2021)*

[3] D. I. Palade, M. Vlad, F. Spineanu, Turbulent transport of the W ions in tokamak plasmas: properties derived from a test particle approach, *Nucl. Fusion 61 116031* (2021)

[4] D.I. Palade, M. Vlad, Fast generation of Gaussian random fields for direct numerical simulations of stochastic transport, *Statistics and Computing* volume 31, Article number: 60 (2021)

Conferences

[1] D. I. Palade, M. Vlad, F. Spineanu, Turbulent transport of the W ions in tokamak plasmas, *IAEA FEC (2021, virtual)*

[2] F. Spineanu, M. Vlad, Analytical instruments that can be useful to plasma theory: axial anomaly, conformal invariance, effective Larmor radius, *19th European Fusion Theory Conference, Padova 11 - 15 oct. 2021 (virtual conf), Poster #50*

[3] D. I. Palade, M. Vlad, F. Spineanu, Direct numerical simulations of the turbulent transport of heavy impurities in tokamak plasma, *19th INTERNATIONAL CONFERENCE ON PLASMA PHYSICS AND APPLICATIONS 2021, Romania.*

[4] M. Vlad, D. I. Palade, F. Spineanu, Computer-aided analysis of the theories of stochastic transport, *19th INTERNATIONAL CONFERENCE ON PLASMA PHYSICS AND APPLICATIONS 2021, Romania.*

[5] A. Croitoru, M. Vlad, F. Spineanu, Nonlinear diffusion of charged particles in pseudo-threedimensional magnetic turbulence, *19th INTERNATIONAL CONFERENCE ON PLASMA PHYSICS AND APPLICATIONS 2021, Romania.*

[6] F. Spineanu, M. Vlad, A.M. Croitoru, Effective Larmor radius, conformal symmetry and the seeds of Edge Localized filaments, *19th INTERNATIONAL CONFERENCE ON PLASMA PHYSICS AND APPLICATIONS 2021, Romania.*

[7] M. Ghiță, D.I. Palade, M. Vlad, Scaling laws of 2D incompressible turbulent transport, *19th INTERNATIONAL CONFERENCE ON PLASMA PHYSICS AND APPLICATIONS 2021, Romania.*

[8] L. Pomârjanschi, D.I. Palade, M. Vlad, Effects of intermittency on turbulent transport in tokamak plasmas, *19th INTERNATIONAL CONFERENCE ON PLASMA PHYSICS AND APPLICATIONS 2021, Romania.*